Virginia Tech Helmet Lab
343 Kelly Hall
325 Stanger St
Blacksburg, Virginia 24061
P: (540) 231-8254
rowson@vt.edu

STAR Methodology for Bicycle Helmets

Megan L. Bland, Craig McNally, and Steven Rowson
Version Date: 5/30/18

Laboratory Tests

An oblique impact drop tower is used to conduct impact testing (Figure 1). A 45° steel anvil produces normal and tangential incident velocities associated with oblique impacts. This angle falls central to a range of reported cyclist head impact angles [1-5]. The anvil is coated with 80-grit sandpaper to simulate road conditions [6], which is replaced after every fourth test. For each test, a helmeted medium NOCSAE headform is positioned in a support ring connected to the drop tower and secured in place with a lever arm that is released just prior to impact. The support ring passes around the outside of the anvil upon impact. No anthropomorphic test device (ATD) neck or effective torso mass is used in this testing, as previous work has suggested that oblique impacts may subject the neck to considerable axial loading, a scenario known to present limited biofidelity for current ATD necks [7-9].

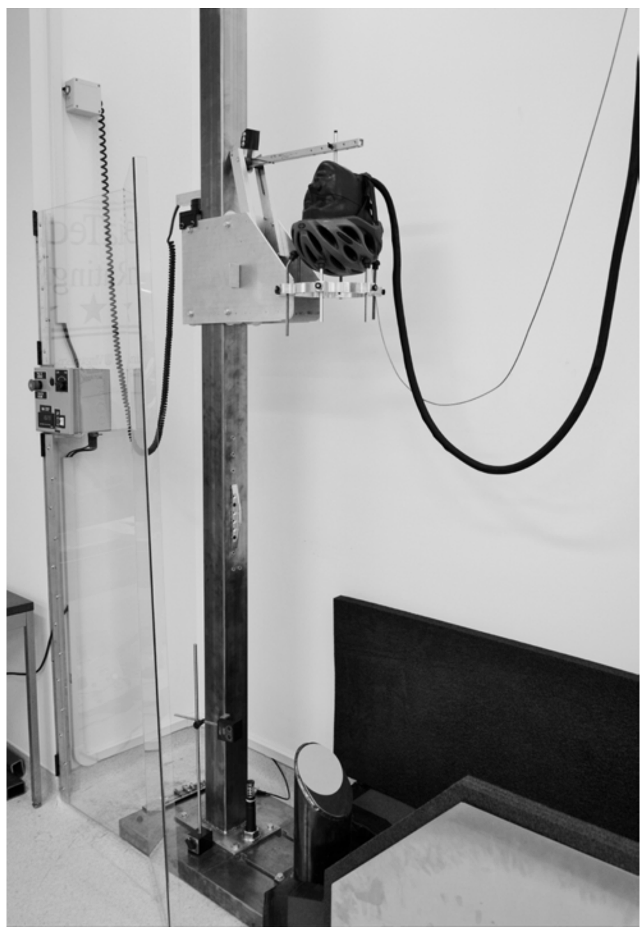

Figure 1. Oblique impact drop tower used for bicycle helmet STAR testing.

Twelve impact conditions are evaluated for STAR testing, including six locations (Figure 2, Table 1) and two velocities (Table 2). Locations are dispersed around the helmet and include two at the rim, a commonly impacted area in cyclist head impacts that is not considered in standards testing [1, 4, 5, 10-16]. To position the helmeted headform, various rods distributed around the support ring are adjusted to move the head into its desired position. The position is specified using a dual-axis inclinometer mounted on a custom holder that fits inside the NOSCAE instrumentation channel, which measures X and Y angles relative to gravity. The inclinometer base faces the neck region of the headform and lays parallel to the base of the headform (2.5° offset from the Frankfort plane). The support ring is also inscribed with 5 degree increments so that Z rotation can be specified as well.

Four samples of each helmet model are subjected to one impact per location (Figure

3), with impact centers set to maintain a minimum distance of 120 mm apart to avoid overlap of damage profiles. Velocities were selected to reflect common cyclist head impact velocities based on helmet damage replication studies [10-11]. Each of the twelve configurations is tested twice, producing a total of 24 impacts per helmet model. Helmets are tested without visors or other extraneous attachments and are fitted in accordance with manufacturer recommendations.

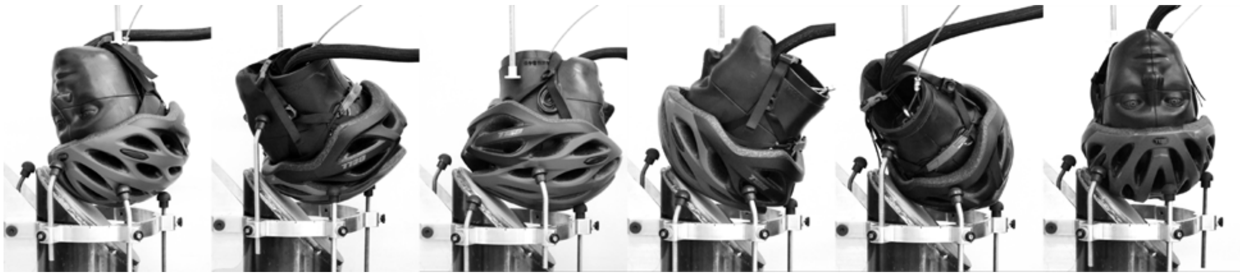

Figure 2. Impact locations 1-6 (left to right). Locations 1, 2, and 6 represent body-driven impacts, in which the head leads the body, locations 3 and 5 represent skidding-type impacts, and location 4 represents an impact from flipping over the handlebars.

Table 1: NOCSAE headform rotations in the support ring for each impact location. X and Y rotations are determined using a dual-axis inclinometer. Z rotation is determined by extending the sagittal line on the NOCSAE face down to the support ring, which is inscribed with 5° increments (headform facing drop tower is 0°, clockwise is positive).

Location	X (deg)	Y (deg)	Z (deg)
1	17.2	1.7	-75
2	-31.4	-13.3	60
3	-22.5	-2.9	-170
4	-7.0	43.7	15
5	-44.0	31.9	180
6	2.6	12.2	-110

Table 2: Prescribed impact velocities for STAR testing, including the resultant, normal, and tangential components. Velocities were chosen based on helmet damage replication data.

Resultant Velocity (m/s)	Normal Velocity (m/s)	Tangential Velocity (m/s)
4.8	3.4	3.4
7.3	5.2	5.2

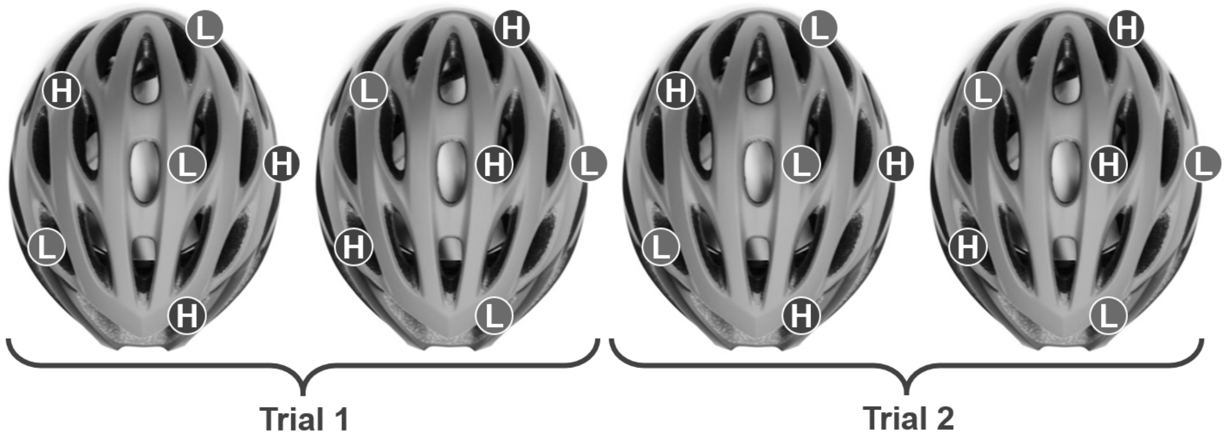

Figure 3. Impact configurations for STAR testing represented on the 4 samples used per helmet model. The superimposed circles represent the six impact locations, with L and H denoting low and high velocities, respectively. Two trials of each location-velocity combination are conducted.

The NOCSAE headform contains three linear accelerometers and a triaxis angular rate sensor (ARS) at the center of gravity to obtain linear and rotational impact kinematics. Data are sampled at 20 kHz and filtered using a 4-pole Butterworth low pass filter with a cutoff frequency of 1650 Hz (CFC 1000) for accelerometer data (SAE J211) and 289 Hz (CFC 175) for ARS data [17]. Peak resultant linear acceleration and peak resultant change in rotational velocity are then determined per test and used to estimate risk of concussion. Risks are averaged together per impact configuration to compute Summation of Tests for the Analysis of Risk (STAR) values.

STAR Ratings

The STAR equation was originally developed to estimate the incidence of concussion that a college football player may experience while wearing a given helmet over the course of one season [18-19]. Common on-field impacts are simulated using laboratory testing, then resulting concussion risk for each impact is estimated and weighted based on the relative frequency that a player might experience that impact scenario during a season of play (termed "exposure"). Bicycle STAR follows a similar ideology wherein common cyclist head impact scenarios are simulated in the laboratory and resulting concussion risks are weighted based on the likelihood of a cyclist experiencing that impact.

The bicycle STAR equation sums the exposure-weighted risks for each impact to generate a single representative concussion incidence value per helmet model. The predicted exposure (E) is determined for each impact location (L) and velocity (V), while concussion risk (R) is computed as a function of the average peak resultant linear acceleration (a) and average peak resultant change in rotational velocity (ω) in each impact configuration (Equation 1).

$$STAR = \sum_{L=1}^{6} \sum_{V=1}^{2} E(L,V) * R(a,\omega) \qquad \text{(Eq. 1)}$$

Exposure weightings were assessed per an assumed 100 cyclist head impacts. Data from helmet damage replication studies were digitized and represented using a cumulative distribution function (CDF) to determine impact velocities and their respective weightings [10-11]. These studies have taken bicycle helmets damaged in real-world accidents and recreated the damage as accurately as possible using laboratory testing, allowing impact velocities to be estimated. Only normal impacts were used in these studies, so velocities and weightings for the STAR ratings were generated based on the normal component of velocity. The 50th and 90th percentile velocities were selected for testing, corresponding to 3.4 and 5.2 m/s normal velocities, respectively (Table 2). Weightings were determined based on the number of impacts that might occur within ±0.5 m/s of these target velocities according to the CDF. Per 100 total head impacts, 38.0 impacts were found to lie in the 3.4 ± 0.5 m/s range and 9.4 impacts in the 5.2 ±0.5 m/s range. The number of impacts were split evenly among the 6 impact locations to yield final weightings (Table 3). Weighting each location equally ensures that helmets are not under-designed in any one location.

Table 3: Exposure values assigned to each location/velocity configuration, which were used as weightings to obtain a STAR value for each helmet.

Location	4.8 m/s	7.3 m/s
1	6.33	1.57
2	6.33	1.57
3	6.33	1.57
4	6.33	1.57
5	6.33	1.57
6	6.33	1.57

Risk of concussion is estimated based on an adaptation of a previously-published multivariate risk function [19]. This function was developed using logistic regression analysis of head impact data from instrumented football players along with associated concussion diagnoses, and incorporates both linear and rotational peak acceleration values. The combination of both linear and rotational kinematics is known to be associated with brain injury [20]. The risk function used for bicycle STAR differs from the previous function by using peak linear acceleration and rotational velocity instead of rotational acceleration. Rotational velocity includes less inherent measurement variability and allows for a duration component of acceleration to be accounted for. Additionally, peak rotational velocity has been shown to be well-correlated to strain development in the brain leading to concussive injury [21-23]. To modify the previous risk function, a published estimated linear relationship between rotational velocity and acceleration was used to replace the rotational acceleration term, resulting in Equation 2 [24].

$$R(a,\omega) = \frac{1}{1 + e^{-(-10.2 + 0.0433 * a + 0.19686 * \omega - 0.0002075 * a\omega)}} \quad \text{(Eq. 2)}$$

The range of final STAR values across helmets are then distributed into a discrete number of stars (1 to 5) for ease of consumer interpretation based on thresholds given in Table 4. The thresholds align with approximate percentage reductions in number of concussions; it is understood that an unhelmeted impact at either of the prescribed impact velocities would always result in injury, so 47.4 concussions and more severe injuries would be sustained based on the exposure weightings of the impacts evaluated (38.0 impacts + 9.4 impacts). The STAR value for each helmet model represents the number of concussions likely to occur out of those 47.4 impacts, which can be expressed as a percentage. The 5, 4, 3, 2, and 1 star ratings align with >70, 70-60, 60-50, 50-40, and <40% reductions, approximately.

Table 4: Thresholds to match STAR values to number of stars in a 5-star rating scale.

STAR Value	Number of Stars
< 14	5
< 19	4
< 24	3
< 29	2
≥ 29	1

References

[1] Verschueren, P. Biomechanical analysis of head injuries related to bicycle accidents and a new bicycle helmet concept, in *Faculteit Ingenieurswetenschappen Departement Werktuigkunde Afdeling Biomechanica en Grafisch Ontwerpen*. 2009, Katholieke Universiteit Leuven: Leuven.

[2] Peng, Y., Chen, Y., Yang, J., Otte, D., and Willinger, R. A study of pedestrian and bicyclist exposure to head injury in passenger car collisions based on accident data and simulations. *Safety Science*, 2012. 50(9): p. 1749-1759

[3] Fahlstedt, M., Baeck, K., et al. Influence of Impact Velocity and Angle in a Detailed Reconstruction of a Bicycle Accident. *IRCOBI Conference*, 2012. 12(84): p. 787-799

[4] Bourdet, N., Deck, C., et al. In-depth real-world bicycle accident reconstructions. *International Journal of Crashworthiness*, 2014. 19(3): p. 222-232

[5] Bourdet, N., Deck, C., Carreira, R.P., and Willinger, R. Head impact conditions in the case of cyclist falls. *Proceedings of the Institution of Mechanical Engineers, Part P: Journal of Sports Engineering and Technology*, 2012. 226(3-4): p. 282-289

[6] ECE. R-22.05: Uniform Provisions Concerning the Approval of Protective Helmets for Drivers and Passengers of Motorcycles and Mopeds. 1999, United Nations Economic Commission for Europe.

[7] In review: Bland, M.L., McNally, C., and Rowson, S. Headform and Neck Effects on Dynamic Response in Bicycle Helmet Oblique Impact Testing. *Proceedings of IRCOBI Conference*, 2018. Athens, Greece.

[8] Sances, A.J., Carlin, F., and Kumaresan, S. Biomechanical analysis of head-neck force in Hybrid III dummy during inverted vertical drops. *Biomedical sciences instrumentation*, 2002. 38: p. 459-464

[9] Rousseau, P., Hoshizaki, T.B., and Gilchrist, M.D. Estimating the influence of neckform compliance on brain tissue strain during a helmeted impact. *Stapp Car Crash Journal*, 2010. 54: p. 37-48

[10] Smith, T. A., Tees, D., Thom, D. R., and Hurt, H. H. Evaluation and replication of impact damage to bicycle helmets. *Accident Analysis & Prevention*, 1994. 26(6), pp. 795-802.

[11] Williams, M. The protective performance of bicyclists' helmets in accidents. *Accident Analysis & Prevention*, 1991. 23(2-3), pp. 119-131.

[12] Ching, R.P., Thompson, D.C., et al. Damage to bicycle helmets involved with crashes. *Accident Analysis & Prevention*, 1997. 29(5): p. 555-62
[13] McIntosh, A., Dowdell, B., and Svensson, N. Pedal cycle helmet effectiveness: A field study of pedal cycle accidents. *Accident Analysis & Prevention*, 1998. 30(2): p. 161-168
[14] Depreitere, B., Van Lierde, C., et al. Bicycle-related head injury: a study of 86 cases. *Accident Analysis & Prevention*, 2004. 36(4): p. 561-567
[15] Bland, M.L., Zuby, D.S., Mueller, B.C., and Rowson, S. Differences in the protective capabilities of bicycle helmets in real-world and standard-specified impact scenarios. *Traffic injury prevention*, 2018. 19(sup1): p. S158-S163
[16] Bland, M.L., McNally, C., and Rowson, S. Differences in Impact Performance of Bicycle Helmets During Oblique Impacts. *Journal of biomechanical engineering*, 2018. 140(9)
[17] Cobb, B.R., Tyson, A.M., and Rowson, S. Head acceleration measurement techniques: Reliability of angular rate sensor data in helmeted impact testing. *Proceedings of the Institution of Mechanical Engineers, Part P: Journal of Sports Engineering and Technology*, 2017. p. 1-6
[18] Rowson, S. and Duma, S.M. Development of the STAR evaluation system for football helmets: Integrating player head impact exposure and risk of concussion. *Annals of Biomedical Engineering*, 2011. 39(8): p. 2130-40
[19] Rowson, S. and Duma, S.M. Brain injury prediction: assessing the combined probability of concussion using linear and rotational head acceleration. *Annals of Biomedical Engineering*, 2013. 41(5): p. 873-82
[20] Ommaya, A.K. Biomechanics of Head Injuries: Experimental Aspects. *Biomechanics of Trauma*, A. Nahum, J. W. Melvin, Ed. Eat Norwalk, CT: Appleton-Century-Crofts, 1985.
[21] Ji, S., Zhao, W., Li, Z., McAllister, T.W. Head impact accelreations for brain strain-related responses in contact sports: a model-based investigation. *Biomech Model Mechanobiol*, 2014. 13(5): 1121-36
[22] Hardy, W.N., Mason, M.J., Foster, C.D., et al. A study of the response of the human cadaver head to impact. *Stapp Car Crash Journal*, 2007. 51:17-80
[23] Kleiven, S. Predictors for Traumatic Brain Injuries Evaluated through Accident Reconstructions. *Stapp Car Crash Journal*, 2007. 51: p. 81-114
[24] Rowson, S., Duma, S.M., et al. Rotational head kinematics in football impacts: an injury risk function for concussion. *Annals of Biomedical Engineering*, 2012. 40(1): p. 1-13